2D/1D AGGRAVATION FACTORS: FROM A COMPREHENSIVE STUDY TO ESTIMATION WITH A NEURAL NETWORK MODEL

Ahmed Boudghene Stambouli, Pierre-Yves Bard, Emmanuel Chaljub, Peter Moczo, Jozef Kristek, Svetlana Stripajova, Capucine Durand, Djawad Zendagui, Boumédiène Derras

16TH EUROPEAN CONFERENCE ON EARTHQUAKE ENGINEERING THESSALONIKI 18 - 21 JUNE 2018

2D/1D AGGRAVATION FACTORS: FROM A COMPREHENSIVE STUDY TO ESTIMATION WITH A NEURAL NETWORK MODEL

Ahmed BOUDGHENE STAMBOULI[1], Pierre-Yves BARD[2], Emmanuel CHALJUB[3], Peter MOCZO[4], Jozef KRISTEK[5], Svetlana STRIPAJOVA[6], Capucine DURAND[7], Djawad ZENDAGUI[8], Boumédiène DERRAS[9]

ABSTRACT

The aim of this paper is to derive "aggravation factors" (AGFs) quantifying the difference between 2D site response and the corresponding 1D estimate for numerous quantities of engineering interest such as response spectra and ten scalar ground motion intensity parameters (GMIPs).
The raw results are a huge collection of AGFs derived by numerical simulation for a total 154692 receivers located at the surface of 894 valleys exhibiting a trapezoidal (131) or triangular (18) shape, with six different velocity contrasts. A simple statistical analysis first allows to identify the respective order of magnitude of these AGFs for each GMIP. In a second step, a neural network approach is used to provide a set of analytical relationships quantifying the coupled effects of a limited number of geometrical and mechanical parameters for all the considered GMIPs, and different positions within the valley. The AGFs are found to be component dependent, with larger values for out-of-plane component (SH waves) compared to the in-plane one (SV waves). They are GMIPs dependent, being the largest for Arias Intensity (I_A) and peak spectral amplification factor (SAF), intermediate for the Cumulative Absolute Velocity (CAV), and the smallest for all the other indicators. The geometry has a significant control on the AGF. For embanked valleys, the highest AGF occur in the center because of constructive interferences, steep edge slopes have significant but very localized effects on the edges, while gentle edge slopes have significant, long distance effects because of their energetic diffraction power. Diffraction away from the lateral slopes also implies a 10-20% variability of the motion on the rocky edges. Finally, results show also that mechanical parameters within the valley do affect the AGF.

Keywords: Aggravation factors, ground motion, numerical simulation, neural networks, 2D valleys.

1 INTRODUCTION

Alluvial valleys or basins are characterized by lateral thickness variations which have been shown to generate peculiar wave propagation phenomena (diffraction of surface waves, possible focusing of body waves, vertical and lateral reverberations) leading to increased wave trapping and interferences, and significant differences (increased duration, generally overamplification, sometimes deamplification) with respect to the case of horizontally stratified layers ("1D soil columns").
Such effects have been qualitatively predicted by theory for about 3-4 decades, and have been actually observed in real recordings or damage distribution (for instance in Kobe in 1995). However, they are only very rarely accounted for even in site-specific studies, because of a) the cost of the required geophysical surveys to constrain the geo-mechanical characteristics of the underground structure not

[1] PhD student, University of Tlemcen/RISAM, Algeria, stambouli_ahmed@yahoo.fr
[2] Scientist, ISTerre, Univ. Grenoble-Alpes/CNRS/IFSTTAR,France, pierre-yves.bard@univ-grenoble-alpes.fr
[3] Scientist, ISTerre, Univ. Grenoble-Alpes/CNRS/IFSTTAR, France, Emmanuel.chaljub@univ-grenoble-alpes.fr
[4] Professor, Comenius University in Bratislava, Slovak Academy of Sciences moczo@fmph.uniba.sk
[5] Professor, Comenius University in Bratislava, Slovak Academy of Sciences kristek@fmph.uniba.sk
[6] PhD student, Comenius University in Bratislava, Slovak Republic, stripajova@fmph.uniba.sk
[7] PhD student, ISTerre, U. Grenoble-Alpes/CNRS/IFSTTAR, France, capucine.durand@univ-grenoble-alpes.fr
[8] Professor, University of Tlemcen/RISAM,Algeria, d_zendagui@mail.univ-tlemcen.dz
[9] Professor, University of Saïda/RISAM, Algeria, b_derras@mail.univ-tlemcen.dz

only underneath but also around the target site, b) the insufficient number of well-documented observations that prevents any statistical treatment for a purely empirical prediction, and c) the lack of comprehensive enough parameter study that would allow to identify the key controlling parameters and to quantify their effects. This was explicitly the goal of a subtask of the NERA EC infrastructure project (2010-2014, www.nera-eu.org) to take advantage in the recent improvements in computing facilities, software accuracy and storage capacity, to perform a large number of computations for a wide variety of geometrical characteristics, velocity contrasts, and receiver locations within the valley, in order to derive statistically meaningful relationships describing the gross dependence of the over-amplification on the main site "meta-parameters". The routine engineering practice to account for effects of subsurface conditions is either to consider the building code provisions based on site classification and the associated pre-defined spectral shapes (most often derived as a function of the "V_{S30}" parameter), or to perform 1D site response studies taking into account the local soil column. Both approaches have in common to be based only on the local soil structure, i.e. implicitly assuming a 1D site response. Therefore, in order to be consistent with the usual practice and to propose the simplest possible procedures to account for subsurface geometry effects, it was decided to quantify their effects only in terms of "aggravation factors (AGFs)" (Chavez-Garcia and Faccioli, 2000; Chavez-Garcia, 2007) describing the ratio between 2D (or 3D) and 1D amplifications for a variety of representative ground motion parameters. Such an approach has been adopted in several recent studies, such as Makra et al. (2001, 2005) for the Euroseistest site (Mygdonian basin, Greece), Paolucci and Morstabilini (2006) for a family of hypothetical basin edges (walls or wedges), Kumar and Narayan (2008), Narayan and Richharia (2008), Hasal and Iyisan (2012), Gelagoti et al. (2012) and Vessia and Russo (2013) for hypothetical basins in the non-linear and linear equivalent cases, and Riga et al. (2016) for a series of partial results obtained within the framework of the NERA project.

The paper successively describes the overall design of the numerical simulations (section 2), an outline of the post-processing from the raw results to the design of neural network models (section 3), and a few examples describing the dependence of the AGFs as a function of the site geomechanical parameters (section 4).

2 NUMERICAL SIMULATIONS

2.1 Overview

The basic idea and goal is to quantify the changes in amplification (increase = overamplification, or decrease = deamplification) compared to the 1D case, and to model their dependence as a function of a limited number of easily available geometrical and mechanical parameters. In that aim, the work was divided in the successive steps listed below:

a) Selection of the models to be computed : geometry, mechanical characteristics, incident wavefield
b) Selection of a representative number of input accelerograms
c) Selection of the (surface) receivers where to compute the resulting motion
d) Selection of the ground motion parameters for which the 2D/1D AGFs are computed.
e) Selection and checks of the numerical simulation software
f) Computations for all the considered cases of the time-domain response for a simple, pulse-like, short-duration signals, in both 2D and 1D cases from each receiver
g) Linear convolution of the pulse response at each receiver l or each valley j with the selected input accelerograms i and derivation of the AGF for each considered ground motion parameter GMP_k: $AGF(R_{ljki}) = GMP_{k\text{-}2D}(R_{lji}) / GMP_{k\text{-}1D}(R_{lji})$
h) Averaging these AGFs over all the considered input accelerograms to derive a mean $AGF_m(R_{ljk})$
i) Using a neural network approach to correlate $AGF_m(R_{ljk})$ to valley geometrical (width, thickness, etc.) and mechanical (velocity profile) characteristics, and also receiver location at valley surface.

This analysis has been done here only in the case of 2D, linear response.

2.2 Design of valley models

2.2.1 Geometric configurations

It was decided to consider a set of trapezoidal and triangular valleys with a broad range of thickness

and widths, and various slope angles on each edge, as indicated in Figure 1. More specifically, a) 6 values are considered for valley width W from 500 m to 20 km, b) 6 values are considered for valley maximum thickness H, from 30 m to 1 km, c) 6 sets are considered for slope angles: 4 symmetrical cases with slope angles equal to 10°, 20°, 45° and 65°, and two non-symmetrical cases with one edge angle at 10°, and the other at 45° or 65°.
In total, this resulted in 149 geometries, as only 27 (H, W) combinations were considered as indicated in Figure 1. Out of them, 131 have a trapezoidal shape, and 18 a triangular shape with a maximum thickness lower than or equal to the H value. The advantages of such a geometry and parameter set are that it is simple, while it allows investigating the effect of the thickness/width "shape ratio" and of the sloping angles on each edge; in addition, a quick survey of the available cross-sections from real valleys indicated that it is not uncommon to have triangular shapes with some dissymmetry. Of course, real alluvial valleys may have more complex geometries, which may require site-specific computations: the present models are simply intended to provide a first order estimate of the expected level of AGFs.

2.2.2 Mechanical characteristics

Considering the large thickness values, velocity profiles with a velocity gradient were considered more realistic. Their functional form is provided in Figure 1: it is controlled by the velocity at surface V_{S0} and at a 1 km depth V_{S1}, and the exponent describing the depth dependence: a value of 0.5 was considered reasonable. The values at surface and depth were then tuned to have V_{S30} values providing integer velocity contrast with the underlying bedrock, which was considered homogeneous with a constant S-wave velocity equal to 1 km/s. The bedrock / sediment surface velocity contrast thus ranges from 2 to 8 (2, 3, 4, 5, 6 and 8). The total number of considered geomechanical cases was thus 894. The damping was tuned to the velocity with the "rule-of-thumb" relation $Q_S = V_S/10$ (i.e., the damping $\varsigma = 0.5/Q_S$ is decreasing with increasing depth). The unit mass was taken as linearly related to the S-wave velocity through the relationship unit mass $\rho(z) = 1600 + 0.6\,(V_S(z) - 100)$ in the sediments, and $\rho_b = 2500$ kg/m^3. The P-wave velocity was taken equal to 1.5 km/s in the sediments (considered as water saturated), and 2 km/s in the bedrock. The quality factor for P-waves was taken according to the following formula : $Q_P(z) = \text{Min}\,(2*Q_S(z), V_P(z)/10)$.

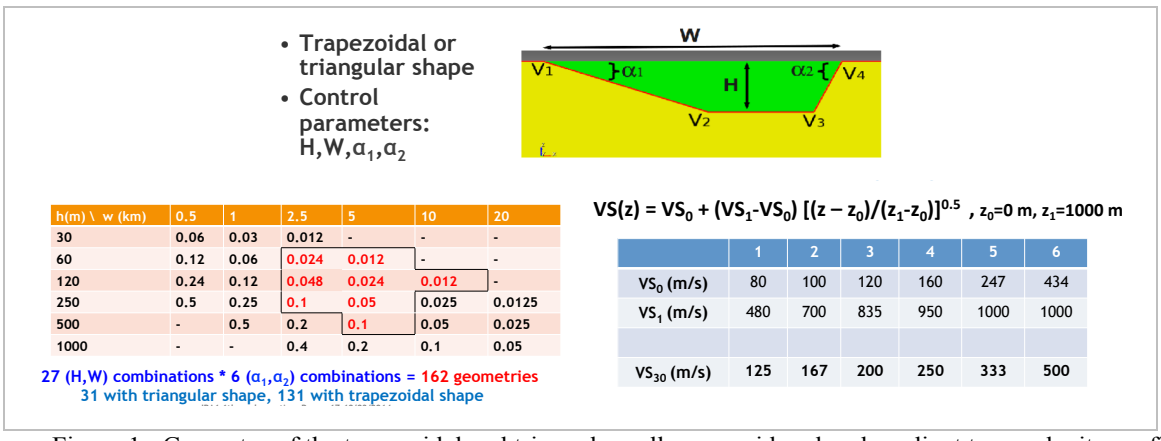

h(m) \ w (km)	0.5	1	2.5	5	10	20
30	0.06	0.03	0.012	-	-	-
60	0.12	0.06	0.024	0.012	-	-
120	0.24	0.12	0.048	0.024	0.012	-
250	0.5	0.25	0.1	0.05	0.025	0.0125
500	-	0.5	0.2	0.1	0.05	0.025
1000	-	-	0.4	0.2	0.1	0.05

	1	2	3	4	5	6
VS_0 (m/s)	80	100	120	160	247	434
VS_1 (m/s)	480	700	835	950	1000	1000
VS_{30} (m/s)	125	167	200	250	333	500

Figure 1 : Geometry of the trapezoidal and triangular valleys considered and gradient type velocity profiles considered for the sedimentary deposit

2.3 Input wavefield and accelerograms

The seismic excitation has been basically defined as vertically incident plane S-waves, in order to provide a meaningful comparison with the routine 1D analysis. The motion may be in-plane (incident "SV" waves) or out-of-plane (incident "SH" waves). As the AGFs are looked for on several ground motion parameters (peak values, response spectra, duration, etc., see below) that are not related linearly with their analog on input motion, it is needed to consider several realistic input accelerograms, in order to get robust estimates on the corresponding average AGFs. Our option has been to select a relatively large set of accelerograms (26) in the RESORCE database (Akkar et al. 2013) on the basis of their frequency contents, as it has been repeatedly shown that amplification

factors of response spectral ordinates are sensitive to the predominant frequency of the input motion: their spectra displayed in Figure 2 indicate that their dominant frequencies span a wide range from around 1 Hz to beyond 10 Hz.

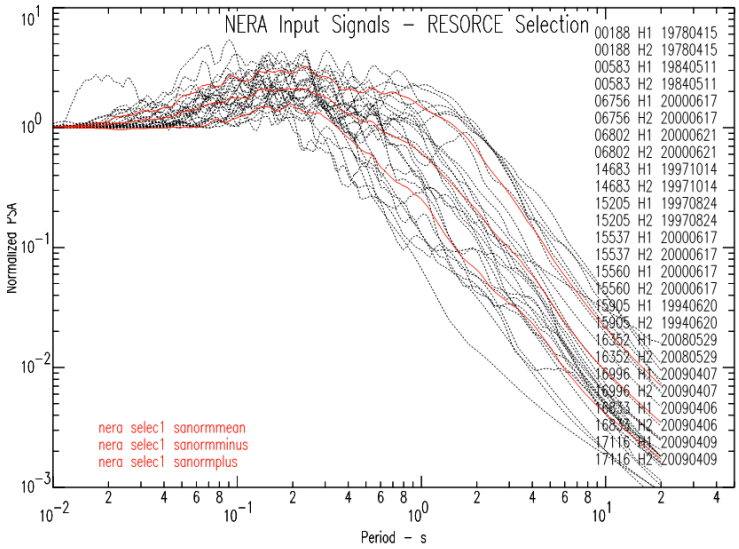

Figure 2 : Normalized response spectra of all the input accelerograms considered (black lines). The solid red curves correspond to the average normalized shape, ± one standard deviation

2.4 Surface receivers

The ground motion has been computed at a minimum of 101 receivers within the valley, with a maximum spacing of 50 m : for valleys having a width smaller than 5km, the receiver spacing thus ranges from 5 m (w = 500 m) to 50 m (w= 5 km), and for valleys wider than 5 km (i.e., 10 or 20 km wide), the number of surface receivers was extended to 200 and 400, respectively. 10 additional receivers have been considered on each side, on the outcropping bedrock, with a spacing equal to w/20 (i.e., from 25 m to 1000 m, over distances from 125 m to 5 km).

2.5 Ground motion intensity parameters

The main ground motion intensity parameter (GMIP) considered in all analysis was the acceleration response spectra at a suite of periods/frequencies. Ten additional, scalar, GMIP were also systematically computed as detailed in Kristek et al. (2018) :

- Peak time domain values (PGA, PGV)
- Short period [Fa, around 0.1 s: geometrical average in the range 0.05 – 0.2 s] and intermediate period [Fv, around 1 s: average in the range 0.5 – 2 s] amplification factors.
- Spectral intensity SI [average in the range 0.10 – 2.5 s], Cumulative Absolute Velocity (CAV), Arias Intensity (I_A), Trifunac-Brady duration D_{TB} (5-95 % and 5-75 %), and root mean square acceleration a_{rms} (5-95 % duration only).

3 COMPUTATION OF THE AGFS AND DERIVATION OF PREDICTIVE MODELS

3.1 Example of "raw results"

The GMIPs listed above have been computed for each receiver and each input accelerogram, in both the 1D and 2D cases. The 2D over 1D AGF (i.e., the ratio of the 2D value over the 1D value) has been computed for each input signal, and then averaged over the whole set of input signals. Both the average and the associated signal-to-signal variability (standard deviation) have been saved. For each receiver, this AGF has been computed as a ratio GMIP(2D)/GMIP(1D), and thus averaged geometrically over the whole set of input accelerograms for all GMIP but the Trifunac-Brady duration D_{TB}, for which the 2D-1D changes have been considered through the duration increase D_{TB}(2D) - D_{TB}(1D), which were then arithmetically averaged over the 26 input accelerograms. Examples of such

averages for some valleys are displayed in Figure 3, providing some hints on the following (mainly qualitative) results:

- The AGFs are parameter dependent: "energy-related" GMIP (I_A, CAV) generally exhibit larger values (up to 3-4), while high-frequency indicators (PGA, 0.1s amplification factor Fa, a_{rms}), exhibit lower values.
- The geometry has a significant control on the AGF :
    - For embanked valleys, the highest AGFs occur in the center because of constructive interferences.
    - Steep edge slopes have large effects (with AGF lower than 1, i.e., deamplification effects), but only locally just over the valley very edges
    - Gentle edge slopes have significant, long distance effects because of their energetic diffraction effect.
- The mechanical characteristics within the valley do affect the AGF:
    - Increase in damping induces decrease of the AGF, especially for high-frequency indicators.
    - The AGF for intermediate to long period GMIP tends to increase with decreasing soil stiffness, but this effect is variable from one geometry to another.

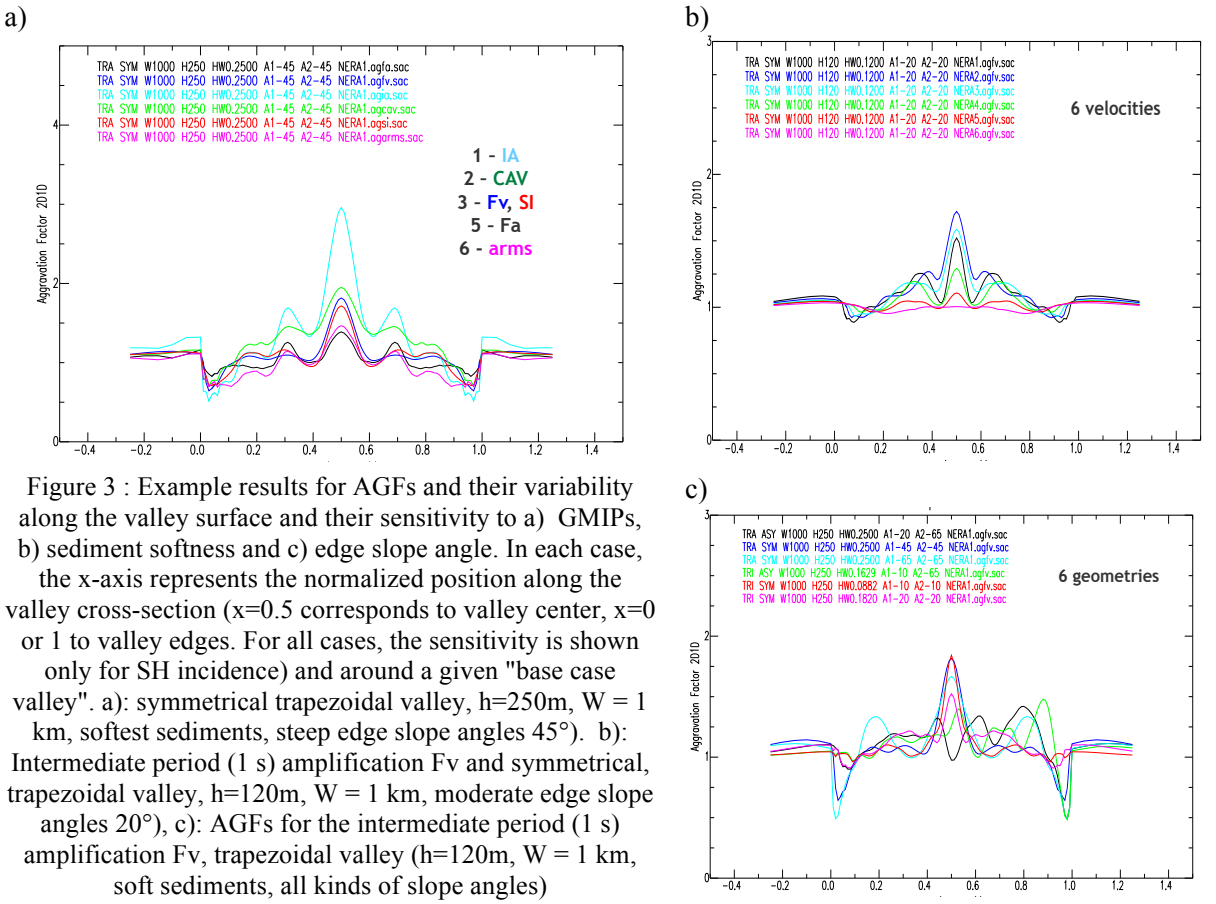

Figure 3 : Example results for AGFs and their variability along the valley surface and their sensitivity to a) GMIPs, b) sediment softness and c) edge slope angle. In each case, the x-axis represents the normalized position along the valley cross-section (x=0.5 corresponds to valley center, x=0 or 1 to valley edges. For all cases, the sensitivity is shown only for SH incidence) and around a given "base case valley". a): symmetrical trapezoidal valley, h=250m, W = 1 km, softest sediments, steep edge slope angles 45°). b): Intermediate period (1 s) amplification Fv and symmetrical, trapezoidal valley, h=120m, W = 1 km, moderate edge slope angles 20°), c): AGFs for the intermediate period (1 s) amplification Fv, trapezoidal valley (h=120m, W = 1 km, soft sediments, all kinds of slope angles)

3.2 Site location: Definition of zones

We obtained a huge collection of average AGFs (about 150000 receivers, 10 severity index + frequency dependent AGFs at 100 frequencies). These AGFs have been archived in summary files with all the needed metadata. In order to propose acceptable AGF to the engineering community, it is needed to establish a simple correspondence between the gross geo-mechanical characteristics of the valley, the site position (near the edge or near the center) and the value of this AGF. For the work presented here, we have characterized the site position at the surface by defining eight (08) different zones as displayed in Figure 4. The total valley width W is first separated in three sub-widths wwe,

wfc and wee, which are the width of the western edge, of the central flat part, and of the eastern edge, respectively.

- wwe = H / tg(α_1)
- wee = H / tg(α_2)
- wfc = max [0, w – H/tg(α_1) – H/tg(α_2)]

The "central flat zone" may have a nul width for gentle slope angles and too large H/w shape ratios: in such cases, the valley is triangular instead of trapezoidal, with a local maximum depth Z_{max} and a position xwe with respect to the western edge given by :

- Z_{max} = w / [1./tg(α_1) + 1./tg(α_2)]
- xwe = w / [1 + tg(α_1) / tg(α_2)]

The 8 zones are then defined as follows:

- BR corresponds to the outcropping bedrock (10 receivers, 5 on each side)
- W2 and W1 are two equal-width zones located over the western (left) slope of the valley; their width is wwe/2 =Min {0.5 H/tg(α_1), 0.5 w/[1+tg(α_1)/ tg(α_2)]}
- Similarly, E2 and E1 are two equal-width zones located over the eastern (right) slope of the valley; their width is wee/2 =Min {0.5 H/tg(α_2), 0.5 w/[1+tg(α_2)/ tg(α_1)]}.
- FW, FC and FE are three equal-width zones located in the central, constant thickness part of the valley. For trapezoidal valleys, such zones may be reduced to one single point, with a local thickness Z_{max}.

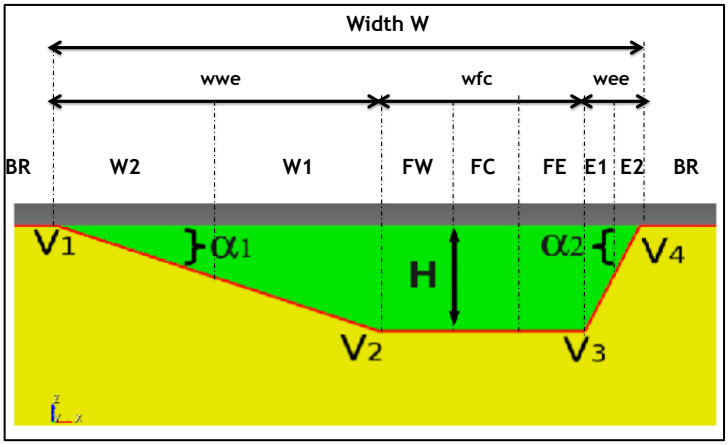

Figure 4 : Definition of valley zones. The total valley width W isseparated in seven zones. Four correspond to the edges above the sloping interface: the extreme edges (W2 and E2), the "inner edges" (W1 and E1). In case of trapezoidal shape, the central, flat part is divided in three equal width parts, FW and FE correspond to the parts closer to the edges ("outer central part"), FC correspond to the central part

Then, for each GMIP and each considered valley (H, w, α_1, α_2 + velocity profile) and a given type of motion (in-plane/SV or out-of-plane/SH), we focus our investigations on the upper envelope of the possible effects, i.e. to consider the maximum AGF over the whole zone and to extract only this value from the archive of simulation results.

- AGAFMAX = zone maximum of the AGF for the amplification factor (ratio of 2D acceleration response spectrum over 1D acceleration response spectrum). This AGAFMAX may occur at different frequencies, but most generally occurs around the site fundamental frequency
- AGPGAMAX = zone maximum of the PGA AGF
- AGPGVMAX = zone maximum of the PGV AGF
- AGFAMAX = zone maximum of the Fa (0.1s amplification factor) AGF
- AGFVMAX = zone maximum of the Fv (1s amplification factor) AGF
- AGSIMAX = zone maximum of the Spectrum Intensity (SI) AGF
- AGCAVMAX = zone maximum of the CAV AGF
- AGIAMAX = zone maximum for the Arias Intensity (I_A) AGF
- AGARMSMAX = zone maximum for the AGF for a_{rms}

- AGDTB1MAX = zone maximum for the Trifunac-Brady duration AGF (5-95%)
- AGDTB2MAX = zone maximum for the Trifunac-Brady duration AGF (5-75%)

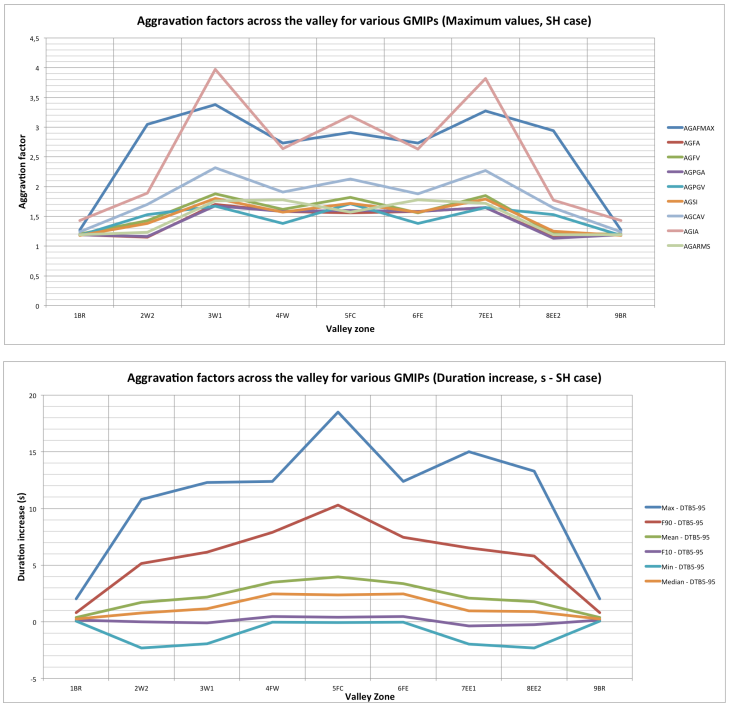

Figure 5 : Variability across the valley of a few statistical values for the various considered GMIP (AGFs on amplification factor for amplitude parameters (top, Fa, Fv, PGA, PGV, SI, CAV, I_A and a_{rms}) and duration (bottom), here only in the out-of-plane/SH case. Top: only maximum values (all cases considered); Bottom: statistical indicators (maximum, mean, minimum, fractiles 90%, 50%, and 10%) for the duration

Minimum and average values of the same quantities were also defined and derived in an analog way. In the present paper however, only the maximum values of each zone are investigated.
A maximum of 894 such values were thus derived for each considered valley (H, w, α_1, α_2 + velocity profile) and a given type of motion (in-plane/SV or out-of-plane/SH). The statistical distribution of these parameters were derived and are presented in Kristek et al. (2015). We simply illustrate here in Figure 5 the dependence of the maximum values of each considered AGF on the zone (amplitude parameters on top and duration increase on bottom), and reproduce the main observations listed in Kristek et al. (2015):

- The "out-of-plane" AGFs are almost systematically larger than the in-plane one. This has been checked for all the amplitude parameters, and is consistent with the results obtained by Moczo et al. (2018) for a set of real valleys
- The largest AGF values correspond to the I_A, the SAF (reaching up to about 4), and the CAV (slightly exceeding a value of 2).
- As to the locations prone to higher AGFs it concerns mainly the inner valley zones, (flat central part + zones W1 and E1).
- A noticeable result from the mean values (not shown here) is the trend to decreased amplitude values on the very edges, especially when the underlying slopes are very steep.
- Finally the duration results indicate duration increase that may significantly exceed 10 s (for signals which are 10 to 30 s long), with a maximum occurring almost systematically in valley center (FE), and a trend to duration decrease on the very edges (zones W2 and E2) (see Figure 5).
- One may notice also non-negligible effects even on the side rock sites: this corresponds to the waves partly reflected in the bedrock on the sloping interface. The mean values are very close to 1, basically from 1.04 to 1.12, but may exceed 1.2 in exceptional cases: such effects are likely contribute to the aleatory variability of ground motion on rock.

3.3 Building neural network models

The goal is to establish simple, approximate relationships providing a satisfactory estimate as the AGFs for different zones in the valley (edge, central part) as a function of the geomechanical characteristics, with a special attention to the short and intermediate period amplification factors Fa and Fv, which are handy to modify the reference spectra. Up to now 7 GMIPs have been considered: I_A, CAV, AFMAX, PGA, PGV, Fa and Fv, as illustrated in Figure 6a.

A special kind of neural network has been selected for this work, the radial basis function (RBF) architecture (Figure 6b). In essence, the RBF approach consists in a "guided interpolation" of the training data, on the basis of the Euclidian distances between a given case and a representative set of all the input data used for the training/learning phase. As usually for neural networks, the architecture consists in an input layer, providing the input values, i.e. the explanatory variables for the model, an output layer with the output value to be predicted (here the AGF), and in-between one "hidden layer" implementing a series of combinations of the input values with an a priori functional form and adjustable weights, and thus providing intermediate values then combined to provide the model output Boudghene Stambouli et al. (2017).. The main elements of the implementation in the present case are provided below:

- The input layer receives the 5-value input vector (X_k) describing the valley geometry (thickness to width ratio hwr = H/w, edge slope angles α_1 and α_2) and site "mechanical parameters (V_{s30} and f_0).
- The output layer corresponds to the value of the considered AGF.
- The hidden layer, i.e. the "processing unit", consists of a limited number of "central neurons" CN_j {j=1, J}, which are 5-value vectors carrying the same information (hwr_j, $\alpha_{1,j}$, $\alpha_{2,j}$, $V_{s30,j}$ and $f_{0,j}$): their values are obtained during the training phase to optimize the sampling of the input vector set.
- The processing for each neuron of the hidden layer consists simply in computing the Euclidian distance between the considered input vector and the considered "central neuron", and deriving the weight w_j to be associated to this key neuron through a "radial basis function" in the form of a Gaussian with a width parameter b_1 to be tuned by the training phase :

$$dist_j = \sqrt{\sum_{k=1}^{5}\left(CN_{j,k} - X_k\right)^2} \qquad \text{and} \qquad w_j = e^{-(dist_j * b1)^2}$$

- The next and last step performed between the hidden and last layer is to combine linearly these Euclidian distance based weights with reference values a_j (to be adjusted in the training phase)

$$AGF_{RBF} = a_0 + \sum_{j=1}^{J}\left(w_j \,.\, a_j\right)$$

A model is therefore characterized by a total of 6 J + 2 free parameters (a_0, b_1, $CN_{j,k}$ and w_j) which are tuned to minimize the root mean square distance between the actual output values of the training set and the model predictions.

3.4 Overview of models and their performance

Such models have been derived for the 7 AGFs indicated in Figure 6a, and for six different zones (4 for the trapezoidal case: FC, FW∪FE, W1∪E1, W2∪E2, and 2 for the triangular case: W1∪E1, W2∪E2). 42 [(4+2)×7] models have thus been derived up to now. Their performance may be "measured" by different indicators such as the reduction of variance between initial AGF values, and the model residuals, or the coefficient of determination between actual AGF values and their predictions. The latter is illustrated in Figure 6c for the 6 zones (abscissa), and the 7 considered parameters (different curves): they are found to range from 0.84 to 94, which are fairly good values, and witness the satisfactory performance of these models to correctly predict the actual AGFs.

4 EXAMPLE MODEL PREDICTIONS

It is not easy to display the functional dependence in case of five input parameters. Given the limited space, only two examples are displayed in Figure 7 and Figure 8. They both display the dependence of the AGF for I_A, for the zone W1UE1 of triangular valleys, and for the central zone FC of trapezoidal valleys, respectively. In every instance, the evolution of the AGF with the "main parameter", i.e., the shape ratio H/w, is displayed, for 8 different parameter combinations: there are 4 curves corresponding

to four different values of one parameter, the three other parameters being constant and equal to some specific fractile value (10%, F10, median, F50, or 90%, F90) as listed in Table 1.

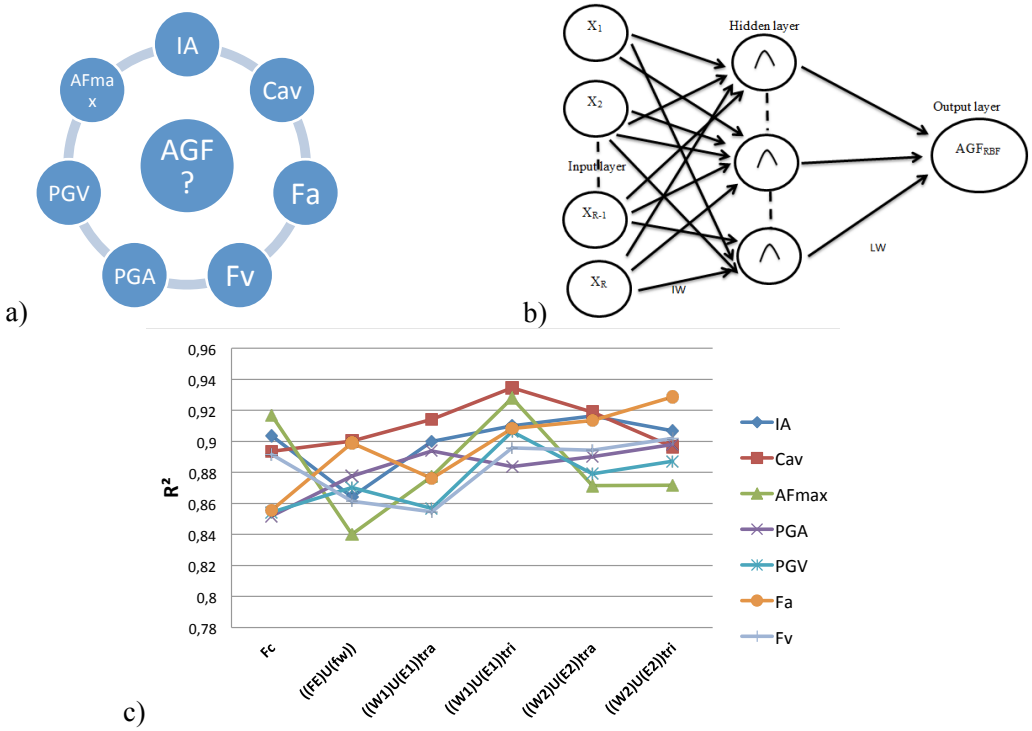

Figure 6 : Neural network analysis: considered AGFs (left), general architecture of a RBF (right) and performance of the 42 different neural networks for the 6 zones and 7 AGFs (bottom)

For the "inner edge" zone in triangular valleys (Figure 7), these plots illustrate the major importance of the shape ratio (AGIA increases with H/w), of the sediment softness (AGIA increases with decreasing velocity), the significant – and somewhat unexpected - effect of the "near" slope angle (α_1) with larger AGFs for lower sloping angles (cases B, C and H), the conversely very limited impact of the "far" slope angle (α_2) (only small differences between cases D and E), and the limited effect of the fundamental frequency (cases F and G). The same conclusions roughly hold also for the central zone of trapezoidal valleys (Figure 8), with a slightly lower impact of the (more distant) sloping angle α_1, and slightly larger impact of the fundamental frequency.

Such conclusions should be considered only as examples of the potentialities of the models obtained with the neural network approach, but they cannot be generalized to AGFs for other parameters. A paper is in preparation that will provide the formulas for each zone and each parameter.

Table 1 : Input parameter values considered for cases displayed in Figures 7 and 8

Plot name	H/w	α_1	α_2	V_{S30} (m/s)	f_0 (Hz)
A	Continuous	Median (15°, *45*°)	Median ` (15°, *45*°)	124, 198, 331, 498	Median (0.5, *0.4*)
B	Continuous	F90 (45°)	Median	Same	Median
C	Continuous	F10 (10°)	Median	Same	Median
D	Continuous	Median	F90 (45°)	Same	Median
E	Continuous	Median	F10 (10°)	Same	Median
F	Continuous	Median	Median	Same	F90 (2.0, *1.4*)
G	Continuous	Median	Median	Same	F10 (0.16)
H	Continuous	10°, 20°, 45°, 65°	Median	Median (240, *220*)	Median

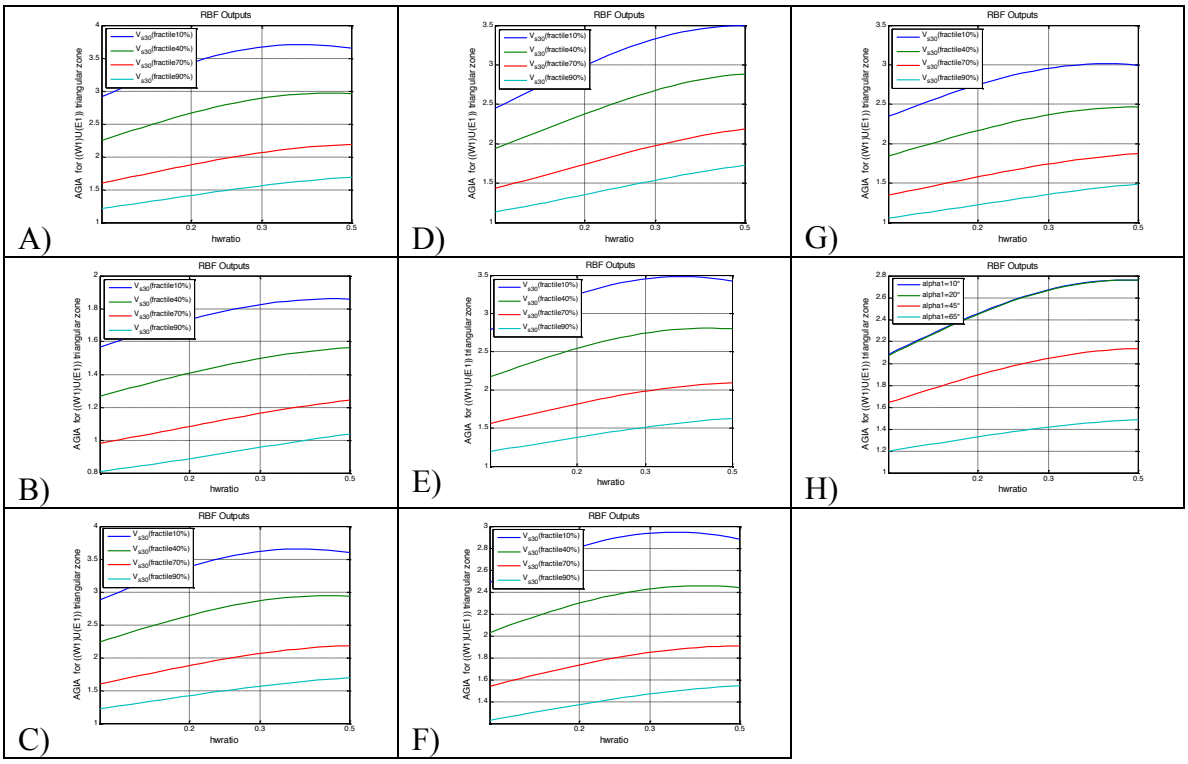

Figure 7 : Example predictions for the Arias Intensity, for the W1UE1 zone in triangular valleys. The different cases considered are listed in Table 1 and explained in the text.

5 CONCLUSIONS

The results from this comprehensive set of computations have been analyzed in a purely statistical way to better understand the key parameters, and modeled using a RBF neural network approach with radial basis function architecture. Both the statistical analysis and the RBF quantitative models lead to the following conclusions:

- The AGFs are component dependent, with larger values for SH, out-of-plane motion compared to SV, in-plane motion. This may be explained by the transfer of energy to the vertical component, as outlined in the other sections of this report
- The AGFs are parameter dependent : they are generally the largest (up to 3-4) for Arias Intensity and the peak spectral amplification factor, intermediate (up to around 2-2.5) for the Cumulative Absolute Velocity, and the smallest (up to 1.5 – 2) for all the other indicators.
- The geometry has a significant control on the AGF.
    - For embanked valleys, the highest AGFs occur in the center because of constructive interferences
    - Steep edge slopes have large effects (with AGFs lower than 1, i.e., deamplification effects), but only very locally just over the valley edges
    - Gentle edge slopes have significant, long distance effects because of their energetic diffraction effect
- The mechanical characteristics within the valley do affect the AGF
    - The AGFs are generally found the largest for the largest velocity contrasts, in relation with the improved efficiency of lateral wave trapping
    - Increase in damping induces decrease of the AGF, especially for high-frequency indicators (not shown here, but obtained from a small, parallel sensitivity study, and supported by the SIGMA results)

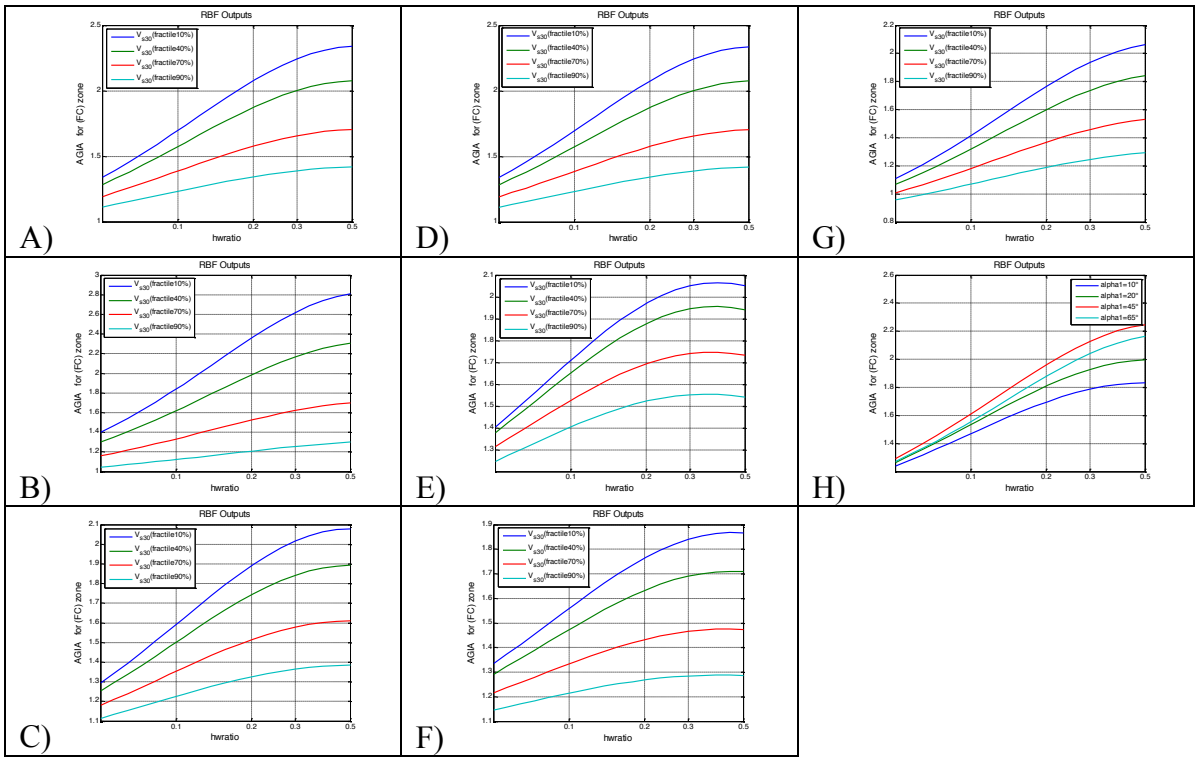

Figure 8 : Example predictions for the I_A, for the FC zone in trapezoidal valleys. The different cases considered are listed in Table 1 and explained in the text

- The ground motion within the valley may be significantly prolongated, up to 10 to 15 seconds.
- The diffraction away from the lateral sloping interfaces implies a slight contamination of the motion on the rocky edges, with an increase of outcropping rock motion, which may be up to 20-30%, especially in the case of steep lateral slopes. This probably contributes to the within-event aleatory variability of rock ground motion

Large AGFs (exceeding 2) in the spectral domain correspond to

- Large velocity contrasts ($V_{S,bedrock}$ /V_{S30} > 5)
- Embankment ratios Z_{max} / Width larger than 0.08
- Sites located within the central, constant thickness part of the valley (zones FW, FC and FE), or very close to it (inner parts of W1 and E1)
- Relatively steep slopes (larger than 20°) when considering sites in the central part of the valley (FW, FC, FE), and any kind of slope angles (including gentle ones) for the "inner-edge" zones W1 and E1.
- In addition, the 42 RBF models developed up to now (7 GMIP, 6 zones) provide simple formulae to estimate the aggravation for each zone and ground motion parameter as a function of a relatively small number of parameters involving the valley geometry (shape ratio h/w, edge slope angles α_1 and α_2, and local mechanical characteristics (V_{S30} and f_0).

One important further step would be to identify, in tight connection with the engineering community, some relevant threshold values for the AGFs on each of the various GMIPs considered here, and to identify the geo-mechanical configurations in which one may expect such thresholds to be exceeded. Another useful contribution would be to compare this set of AGFs corresponding to "virtual", simple shaped valleys, with those derived for real valleys (Moczo et al., 2018).

6 ACKNOWLEDGMENTS

The simulation work has been funded by the European Commission FP7 under the Grant Agreement No 262330 (NERA Project, www.nera-eu.org/), and and also by the Slovak Research and

Development Agency under the contracts APVV-15-0560 (project ID-EFFECTS). The neural network part was supported by the project: “Prédiction du mouvement sismique et estimation du risque sismique lié aux effets de site” 13MDU901 Tassili CMEP between Universities of Tlemcen (Algeria) and Grenoble (France).

7 REFERENCES

Akkar S, Sandıkkaya MA, ¸Senyurt M, Azari AS, Ay BÖ, Traversa P, Douglas J, Cotton F, Luzi L, Hernandez B, Godey S (2013c) Reference database for seismic ground-motion in Europe (RESORCE). Bull Earthq Eng. doi:10.1007/s10518-013-9506-8.

Boudghene Stambouli, A., Zendagui, D., Bard, P.-Y. and Derras, B., 2017. Deriving amplification factors from simple site parameters using generalized regression neural networks: implications for relevant site proxies, Earth, Planets and Space (2017) 69:99, DOI 10.1186/s40623-017-0686-3

Chávez-García, FJ and E Faccioli (2000) Complex site effects and building codes: Making the leap. Journal of Seismology 4: 23–40, 2000. Kluwer Academic Publishers.

Chávez-García, FJ (2007) Site effects: from observation and modelling to accounting for them in building codes. In: Pitilakis KD (ed.), Earthquake Geotechnical Engineering, Springer, 53-72.

Gelagoti F, Kourkoulis R, Anastasopoulos I, Gazetas G (2012) Nonlinear dimensional analysis of trapezoidal valleys subjected to vertically propagating SV waves. B Seismol Soc Am 102: 999-1017

Hasal M, Iyisan R (2012) Effect of edge slope on soil amplification at a two dimensional basin model. 15th WCEE, Lisbona, Paper, (4455)

Kristek, J., P. Moczo, P.-Y. Bard, F. Hollender, S. Stripajová, Z. Margočová, E. Chaljub et C. Durand, 2015. Identification of key site features for site effect evaluation: extensive numerical sensitivity studies of sedimentary basin structures. Sigma deliverable D3-151, Mai 2015, 217 pages.

Kristek, J., P. Moczo, P., P.-Y. Bard, F. Hollender and S. Stripajová (2018). Computation of amplification factor of earthquake ground motion for a local sedimentary structure, Bull Earthquake Eng., accepted, in press.

Kumar S, Narayan JP (2008) Importance of quantification of local site effects based on wave propagation in seismic microzonation. J Earth Syst Sci 117: 731-748

Makra K, Chávez-García FJ, Raptakis D, Pitilakis K (2005) Parametric analysis of the seismic response of a 2D sedimentary valley: implications for code implementations of complex site effects. Soil Dyn Earthq Eng 25: 303-315

Makra K, Raptakis D, Chávez-García FJ, Pitilakis K (2001) Site effects and design provisions: the case of Euroseistest. PAGEOPH 158.

Moczo, P., J. Kristek, P.-Y. Bard, S. Stripajová, F. Hollender, Z. Chovanová, M. Kristekova and D. Sicilia, 2018. Key structural parameters affecting earthquake ground motion in 2D and 3D sedimentary structures. Bull. Earthquake Engineering, under revision.

Paolucci R, Morstabilini L (2006) Non-dimensional site amplification functions for basin edge effects on seismic ground motion. In: Third International Symposium on the Effects of Surface Geology on Seismic Motion. 30. Grenoble, France, August 30 - September 1, 2006, pp. 823-831

Narayan J, Richharia AA (2008) Effects of strong lateral discontinuity on ground motion characteristics and aggravation factor. J Seismol 12: 557-573

Riga E, Makra K, Pitilakis K (2016) Aggravation factors for seismic response of sedimentary basins: A code-oriented parametric study. Soil Dyn Earthq Eng 91: 116-132

Vessia G, Russo S (2013) Relevant features of the valley seismic response: the case study of Tuscan Northern Apennine sector. B Earthq Eng 11: 1633-1660